Structural and mechanistic studies of enolase

George H Reed, Russell R Poyner, Todd M Larsen, Joseph E Wedekind* and Ivan Rayment

The high-resolution structure of yeast enolase cocrystallized with its equilibrium mixture of substrate and product reveals the stereochemistry of substrate/product binding and therefore the groups responsible for acid/base catalysis and stabilization of the enolate intermediate. Expression and characterization of site-specific mutant forms of the enzyme have confirmed the roles of amino acid side chains in the catalysis of the first and second steps of the reaction. Coordination of both required magnesium ions to the carboxylate of the substrate/product indicates a role for these cations in stabilization of the intermediate.

Addresses
The Institute for Enzyme Research, Graduate School, and Department of Biochemistry, College of Agricultural and Life Sciences, University of Wisconsin–Madison, Madison, WI 53705, USA
*Department of Structural Biology, Fairchild Center, Stanford University School of Medicine, Stanford, CA 94305-5400, USA

Current Opinion in Structural Biology 1996, 6:736–743

Abbreviations

EPR	electron paramagnetic resonance
PEG	polyethylene glycol
P-enolpyruvate	phosphoenolpyruvate
2-PGA	2-phospho-D-glycerate
PhAH	phosphonoacetohydroxamate
TSP	tartronate semialdehyde phosphate

Introduction

Enolase catalyzes the reversible dehydration of 2-phospho-D-glycerate (2-PGA) to give P-enolpyruvate during glycolysis. The recent availability of high-resolution structural data on enolase–substrate complexes makes it possible to correlate structure with the enzymatic characteristics of enolase and of various site-specific mutant forms of this protein. This review will focus on developments within the past year that pertain to the structure and mechanism of enolase and which cover a small sampling of the extensive work on enolase. Readers are referred to the references contained in the recent papers for a more comprehensive view of enolase.

Background

Isotope-exchange studies suggest that enolase catalyzes the β-elimination reaction in a stepwise manner wherein OH^- is eliminated from C3 of a discrete carbanion (enolate) intermediate [1,2]. This intermediate is created by removal of the proton from C2 of 2-PGA by a base in the active site. This stepwise model (Fig. 1) of the reaction is also supported by other lines of investigation [3,4].

The C2 proton of 2-PGA has a $pK_a > 30$ whereas enzymic bases have pK_as at least 20 pK_a units lower. The catalytic turnover of yeast enolase ($80\ s^{-1}$) indicates that the ΔpK_a must be reduced substantially in the active site. Hence, there is considerable interest in understanding the means by which enolase accomplishes this difficult ionization step. The second step in the reaction, elimination of OH^- from the intermediate, is also expected to require assistance in the form of general-acid catalysis. Indeed, measurements of isotope effects on the overall reaction indicate that formation of the intermediate is not the major limitation to the rate [1,2,5]. The kinetic mechanism is ordered with respect to the addition of 2-PGA and the second Mg^{2+} [6]. Mg^{2+} adds last, such that the inhibition that is observed at high concentrations of Mg^{2+} is probably due to slower release of product [6]. The overall equilibrium constant is ~4 and the equilibrium constant on the enzyme is approximately unity [7].

Stereochemical investigations established that the β-elimination reaction catalyzed by enolase is *anti* [8]. The stereochemical results indicate that the groups responsible

Figure 1

Stepwise model for the β-elimination reaction of enolase. A, acid; EB, enzymic base.

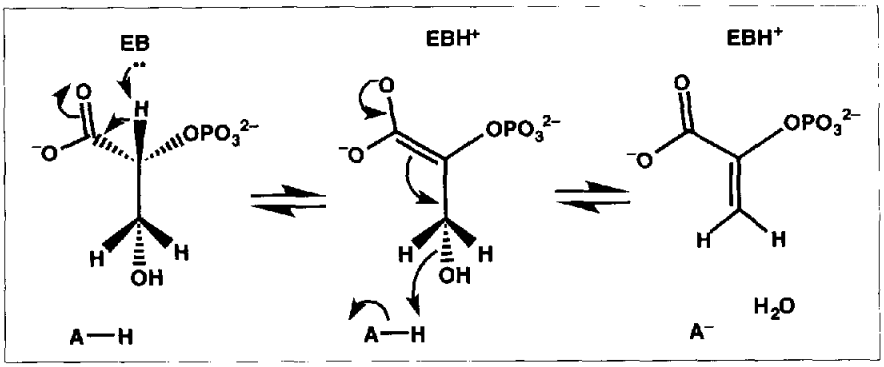

for general-base and general-acid catalysis lie on opposite surfaces of the active site.

Another important property of enolase is its requirement for activation by two equivalents of divalent-metal ion per subunit [9]. Early electron paramagnetic resonance (EPR) experiments with Mn^{2+} complexes of enolase indicated that the two metal ions were bound sufficiently close to each other to undergo spin-exchange coupling [10]. More recently, EPR measurements of Mn^{2+} enolase complexes and the potent inhibitor phosphonoacetohydroxamate (PhAH) and ^{17}O labeled forms of PhAH established a bichelate structure of the inhibitor in which the carbonyl oxygen of the hydroxamate was a μ-bridging ligand (Fig. 2) [11]. These spectroscopic results were confirmed by a 2.1 Å resolution X-ray structure of the cocrystallized complex of $(Mg^{2+})_2$–PhAH–enolase [12].

Figure 2

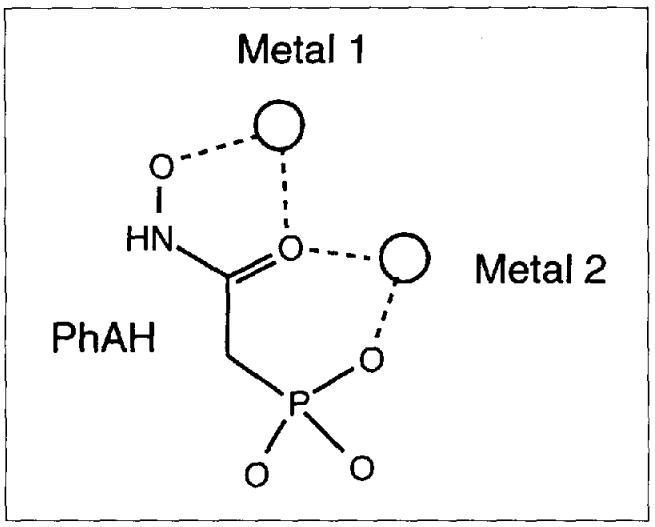

Schematic model of the bichelate metal complex of the inhibitor, PhAH, in the active site of enolase. Charges on the metal ions and PhAH are omitted for simplicity.

Structure of enolase

Type I enolase from yeast has 436 amino acids per subunit. In yeast and most higher organisms enolase subunits assemble into dimers. The primary structure of enolase is highly conserved. Each subunit consists of an N-terminal and a C-terminal domain [13]. The latter folds into an α/β barrel having an atypical connectivity of $\beta_2\alpha_2(\beta\alpha)_6$ [13]. The active site is located in a cavity at the C-terminal ends of the barrel strands. A ribbon representation of one subunit of the $(Mg^{2+})_2$–enolase2-PGA complex [14••] is shown in Figure 3. The N-terminal domain contributes a long flexible loop that closes on the active site via chelation of Ser39 to one of the divalent cations [12]. This loop closure, and movement of another loop containing His159, constitute the major conformational changes that occur in response to binding of substrates or inhibitors in the active site [12,14••].

Active site

Some of the several acidic and basic residues that line the active site are highlighted in the view of the Mg^{2+}–enolase complex shown in Figure 4 [15]. An earlier structure of the substrate/product complex was obtained by soaking substrate into crystals of Mg^{2+}–enolase at pH 6 in 3 M $(NH_4)_2SO_4$ [16]. This structure revealed electron density for the substrate/product in the active site. Modeling of 2-PGA into the density suggested that the carboxylates from Glu168 and Glu211 and an intervening water might serve as the base catalyst [16]. This early structure, however, lacked the second equivalent of Mg^{2+}, and electron density was ambiguous with respect to the positions of the carboxylate and hydroxymethyl moieties of the substrate. Moreover, the structure of the *bis* Mg^{2+} complex with PhAH indicated that Lys345, on the opposite face of the active site, was a viable candidate for the base catalyst [12].

The recent structure of $(Mg^{2+})_2$–enolase–2-PGA/P-enolpyruvate was obtained for crystals of the complex cocrystallized at pH 8 from PEG [14••]. In contrast to the previous structure [16], difference electron density corresponding to the substrate/product was unambiguous with respect to the stereochemistry of substrate binding, and the coordination schemes of both essential magnesium ions was clear. Figure 5 shows the active site with bound 2-PGA and the residues that are in position to participate in catalysis. An intricate coordination of the magnesium ions to the substrate/product is an intriguing revelation of this structure. The carboxylate of the substrate/product coordinates in a bidentate manner to the higher affinity Mg^{2+} ion. One of the carboxylate oxygens bridges to the second Mg^{2+} ion, and is therefore structurally analogous to the carbonyl oxygen in PhAH [12]. The second Mg^{2+} ion also coordinates to an oxygen from the phosphate of the substrate/product (Fig. 6). The ε-amino group of Lys396 is also within hydrogen-bonding distance of a carboxylate oxygen. The magnesium ions and a protonated ε-amino group of Lys396 are the agents that are in position to stabilize the increased negative charge that develops on the carboxylate in the enolate intermediate. The hydroxymethyl moiety of 2-PGA points towards the carboxylate of Glu211, and Lys345 is positioned near the C2 proton of 2-PGA.

A third proposal for the general-base catalyst of enolase emerged from a structure of the enolase from lobster muscle [17]. This scheme was based on assignment of electron density for the weak inhibitor phosphoglycolate, which was soaked into crystals in concentrated $(NH_4)_2SO_4$. Like the $(NH_4)_2SO_4$ crystals of the yeast enzyme [16], these crystals lacked the second divalent-metal ion. The suggestion from this structure that His159 (using the yeast numbering system) functions in general-base catalysis is

Figure 3

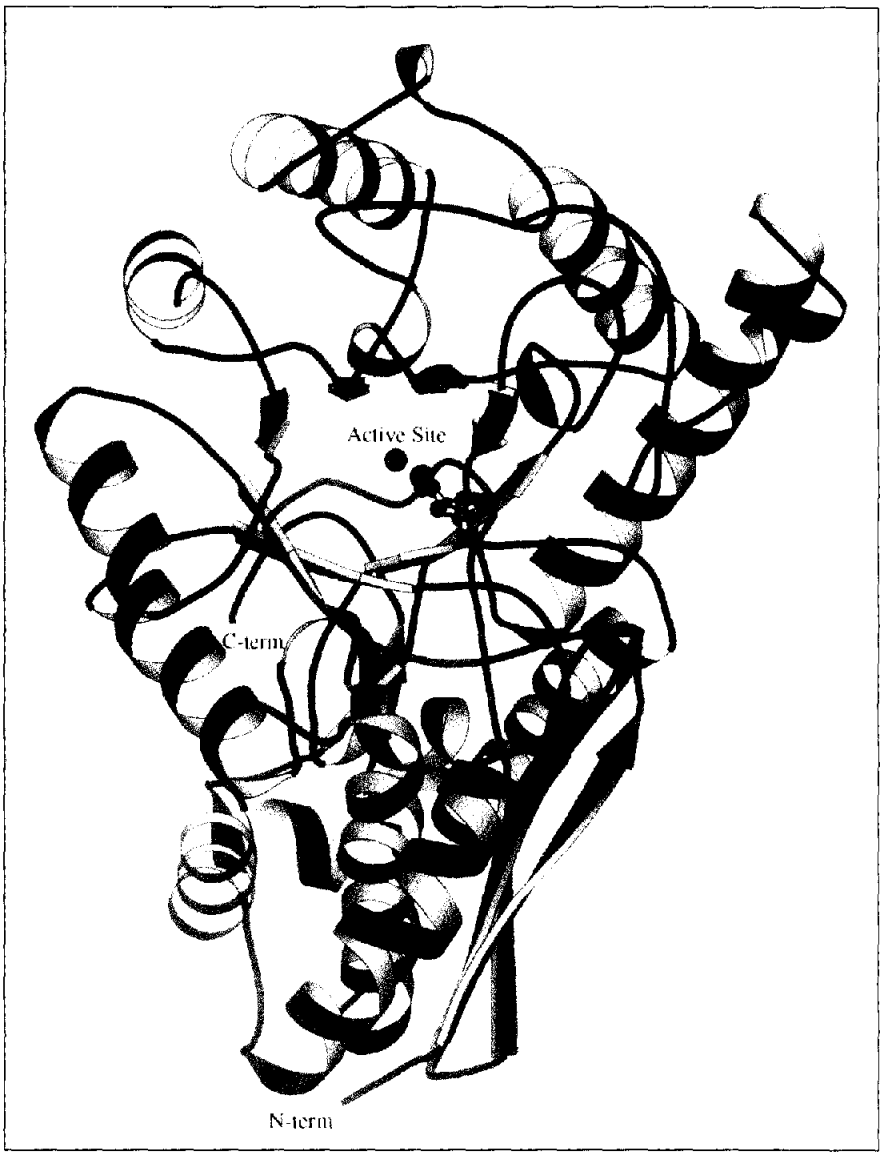

Ribbon representation of a subunit of the enolase–$(Mg^{2+})_2$–substrate/product complex [14••]. The N-terminal domain is shown in green and the C-terminal domain is shown in blue. Magnesium ions are represented by spheres and a ball and stick model of 2-PGA is shown in the active site. X-ray coordinates for this structure are deposited in the Brookhaven Protein Data Bank (entry code 1ONE). Figure drawn using MOLSCRIPT [25].

inconsistent with the stereochemistry of the structure of the cocrystallized substrate/product complex [14••] as well as with the facile exchange of the C2 proton of 2-PGA with solvent [1,2].

Site-specific mutagenesis

The various proposals for residues involved in acid/base catalysis in enolase can be tested by site-specific mutagenesis. As might be anticipated from the strict conservation of residues in the active site of enolase, mutation of any of four residues (Glu168, Glu211, Lys345, Lys396) in the active site of enolase lowers the activity in the overall reaction relative to wild-type enolase by a factor of 10^4–10^5 (Table 1). The stepwise nature of enolase catalysis (Fig. 1) facilitates evaluation of the catalytic properties of mutant forms of the enzyme, because variants that are inactive in the overall reaction may retain activity in one of the steps. For example, one can expect that mutant proteins that retain the base should also retain the ability to catalyze the first step in the reaction cycle, or an analog of this step such as ionization of the inhibitor (TSP; Fig. 7).

Glu168Gln and Gln211Gln enolases have been expressed in an enolase type I knockout strain of yeast [18,19•] and in *Escherichia coli* [20••]. Expression of mutant forms of yeast enolase in *E. coli* leads to a more tractable purification than with the yeast system, in which type II enolase and type II/mutant type I hybrids are present. Indeed lower activities are reported for Glu168Gln and Glu211Gln enolases obtained from the *E. coli* expression system [20••]. Both Glu168Gln and Glu211Gln enolases catalyze the TSP ionization as assayed by UV difference spectroscopy, although at rates lower than wild-type enolase [18,19•,20••].

Figure 4

Ribbon representation of the active site of the enolase–Mg^{2+} complex [15]. Coordination of Mg^{2+} (green sphere) to the three carboxylate ligands and oxygens (red spheres) of the three water ligands is shown. Important active-site residues (denoted using amino acid single-letter code) are represented as ball and stick models. The active-site loop in its open conformation is shown in green. X-ray coordinates for this structure are deposited in the Brookhaven Protein Data Bank (entry code 1ebh). Figure generated using the program MOLSCRIPT [25].

Table 1

Kinetic constants of yeast enolase and variants.

	2-PGA Dehydration		$^1H/^2H$ Exchange of 2-PGA	Hydration of (Z)-3-Cl-P-enolpyruvate	References
Yeast enolase	K_M (mM)	k_{cat} (s^{-1})	k_{ex}/k_{cat}	k_{cat}(s^{-1})	
Wild type	0.30 ± 0.06	78 ± 4	0.23 ± 0.006	> 0.05	[2,20••]
Lys345Ala	0.7 ± 0.1	(6.3 ± 0.4) × 10^{-4}	< 0.5	(8.8 ± 0.7) × 10^{-4}	[20••]
Lys345Met	0.027 ± 0.003	1.4 × 10^{-3}	–	–	(a)
Glu211Gln	0.12 ± 0.02	(6.6 ± 0.3) × 10^{-4}	(2.0 ± 0.1) × 10^3	(8.8 ± 0.7) × 10^{-6}	[20••]
Lys396Met	0.10 ± 0.02	3.0 × 10^{-3}	–	–	(b)
His373Asn	0.011 ± 0.002	8.4	–	–	(b)
Glu168Gln	0.11 ± 0.04	(4.0 ± 0.4) × 10^{-4}	(2.5 ± 0.2) × 10^3	(2.3 ± 0.3) × 10^{-4}	[20••]

(a) RR Poyner, V Bandarian, GH Reed, unpublished data. (b) RR Poyner, LT Laughlin, GH Reed, unpublished data.

The exchange of the C2 proton of 2-PGA with solvent deuterons is a more direct assay of the viability of the catalytic base, and this reaction is conveniently assayed by NMR spectroscopy. Assays of the Glu168Gln, Glu211Gln, and Lys345Ala enolases in this exchange reaction revealed that Glu211Gln and Glu168Gln enolases were capable of catalyzing this exchange whereas no exchange activity could be detected with Lys345Ala enolase [20••]. With Glu211Gln enolase, exchange was essentially complete prior to the appearance of P-enolpyruvate in the reaction

Figure 5

Stereoview of the active site of the enolase–$(Mg^{2+})_2$–substrate/product complex [14••]. The Cα backbone is shown as a blue tube; the magnesium ions are represented as green spheres; catalytic groups (denoted using amino acid single-letter code) are shown as ball and stick models in grey, and the ball and stick model of 2-PGA is highlighted with yellow bonds. Figure generated using the program MOLSCRIPT [25].

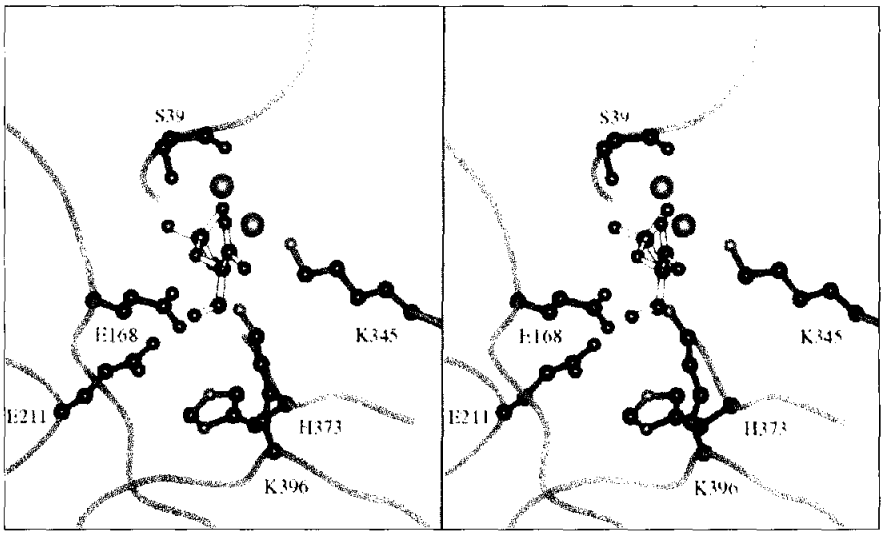

Figure 6

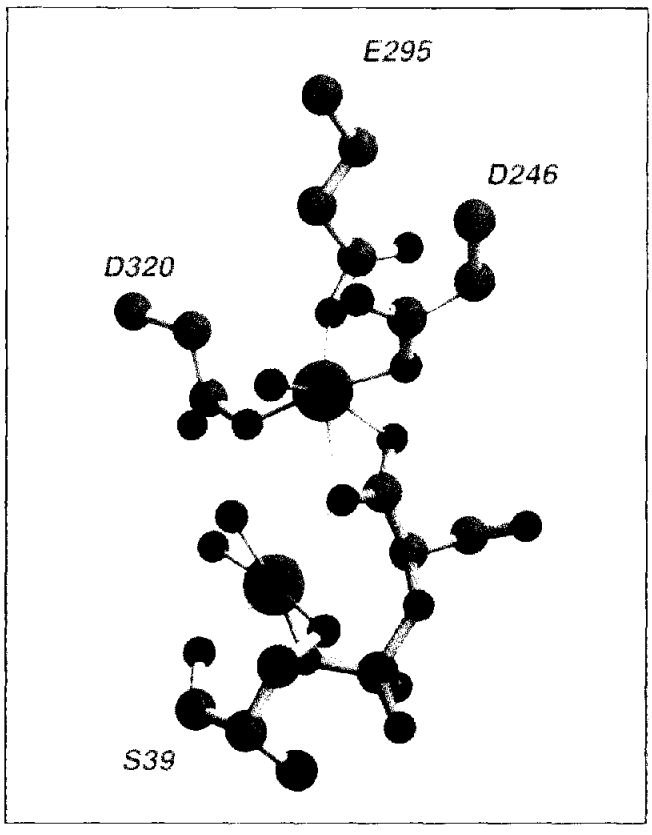

The active site of the enolase–$(Mg^{2+})_2$–2-PGA complex showing coordination of the magnesium ions [14••]. Active-site residues are denoted using amino acid single-letter code. Figure generated using MOLSCRIPT [25] and Raster3D [26,27].

Figure 7

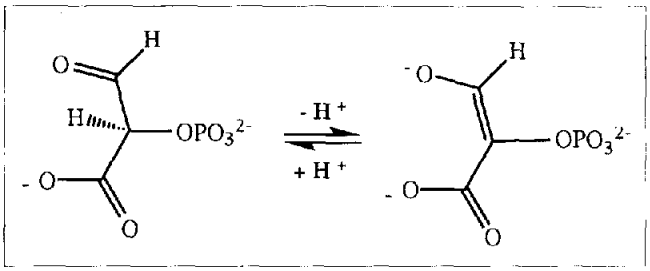

Ionization of the inhibitor tartronate semialdehyde phosphate.

mixture. This observation reinforces the proposal that the enolase reaction is indeed stepwise. Recent assays of Glu211Gln enolase indicate that with Mg^{2+}, $k_{exchange}$ is comparable to the overall catalytic turnover, k_{cat}, of wild-type enolase (PK Hall, RR Poyner, GH Reed, unpublished data). The failure of Lys345Ala enolase to catalyze the H/D exchange in 2-PGA is consistent with the recent X-ray structure which shows that the C2 proton of 2-PGA is directed towards the ε-amino moiety of Lys345 [14••].

The enolase-catalyzed hydrolysis of the (Z) isomer of C3-halogenated analogs of P-enolpyruvate to form the enol of TSP (Fig. 8) [21] provides a means to assay the viability of groups in mutant forms of enolase which activate water in the reverse reaction [20••]. This reaction involves addition of OH^- and elimination of X^- (where X = F or Cl) at C3 of the analog and probably includes an intermediate which is structurally analogous to the enolate of 2-PGA. The product of this reaction (a form of TSP) is a potent inhibitor of enolase, and single-turnover assays were therefore employed. The order of effectiveness in this reaction, wild type > Lys345Ala > Glu168Gln >> Glu211Gln, suggested that Glu211 is important in activation of water and therefore might function in acid/base catalysis of the second step of enolase catalysis [20••]. This suggestion was borne out by the X-ray structure, which exhibited well defined electron density for the hydroxymethyl of 2-PGA

Figure 8

The enolase-catalyzed hydrolysis of the (Z) isomer of C3-halogenated analogs of phosphoenolpyruvate.

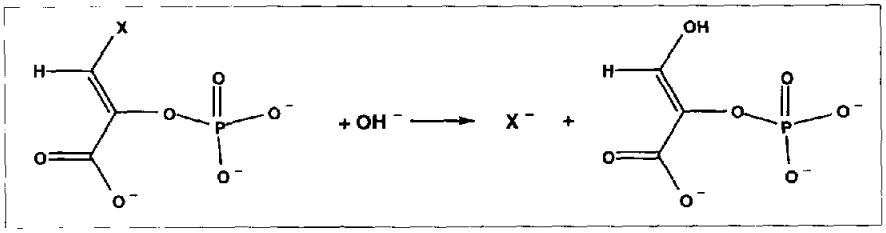

Figure 9

Schematic model of enolase catalysis.

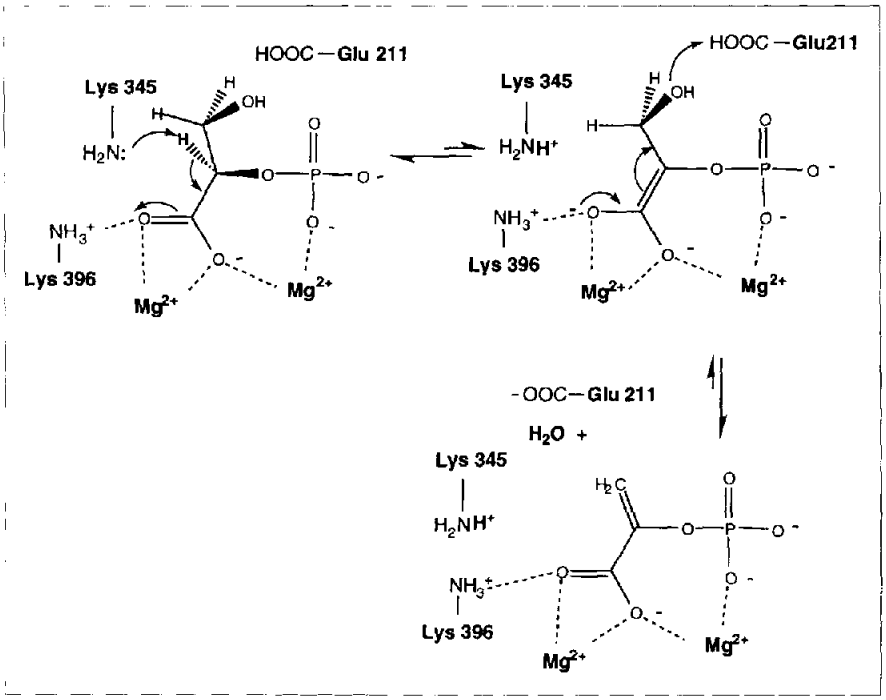

directed towards Glu211 (Fig. 5) [14••]. The imidazole side chain of His373 is also near the hydroxymethyl moiety, and the potential for participation by this side chain is still feasible. Assays of highly purified His373Asn enolase (RR Poyner, GH Reed, unpublished data) show that this mutant enzyme retains ~10% of wild-type activity (Table 1); therefore, His373 is not essential for effective catalysis.

Results from X-ray crystallography on the equilibrium mixture of enolase [14••] and from assays of the glutamate and lysine mutant forms of enolase (Table 1) [20••], show that the ε-amino of Lys345 and the carboxylate of Glu211 function in general-base and general-acid catalysis, respectively, in the forward reaction of enolase. A protonated ε-amino of Lys396 is within hydrogen-bonding distance from a carboxylate oxygen and probably participates with the magnesium ions in stabilizing the enolate intermediate. Lys396Met enolase is lower in activity by $>10^4$ compared with wild-type enolase (RR Poyner, LT Laughlin, GH Reed, unpublished data). The side chain of Glu168, which is in position to interact with Glu211 and with Lys396, is likely to be important in both steps of catalysis, and this suggestion is confirmed by the properties of Glu168Gln enolase (Table 1) [20••]. Ser39 in the active-site loop is also critical for efficient catalysis. Ser39Cys enolase is more active with Zn^{2+} ions than with Mg^{2+} ions, but activity is $<10^{-3}$ wild type (AM Langner, LT Laughlin, RR Poyner, GH Reed, unpublished data).

Schematic model of enolase catalysis

The structural results and results from mutant forms of enolase are consistent with the mechanism shown in Figure 9.

The pK_a of Lys345 is not yet known, but it is apparent that the intricate coordination of the carboxylate to the magnesium ions and the interaction of the carboxylate oxygen with Lys396 must lower the pK_a of the C2 proton to allow ionization at a rate compatible with turnover. There

is chemical precedent for chelation-induced acidification of α protons [22].

Model calculations have been published on possible environmental influences on the pK_a of the C2 proton of 2-PGA [23]. In spite of missing the important interactions between the substrate carboxylate and both Mg^{2+} ions, these calculations predict that a conformation that is compatible with enolate formation is most favorable. These predictions reconfirm what has been expected — namely that the enolate is the most stable form of the carbanion intermediate [3]. The fact that enolase binds the carboxylate of 2-PGA in the proper conformation for enolate formation probably reduces the 'intrinsic' barrier to ionization of the carbon acid.

Conclusions

The recent work on enolase explains many of the fundamental characteristics of the enzyme. The properties of various mutant forms of enolase in partial reactions reinforce the concept of a stepwise mechanism. The acid/base catalysts are on opposite faces of the active site, which is in harmony with the *anti* stereochemistry of the elimination. Direct coordination of both metal ions to the carboxylate moiety of the substrate explains the *bis* metal ion requirement for catalysis and the magnetic properties of paramagnetic complexes. One can anticipate that more detailed information on the properties of the binuclear-metal center in enolase complexes, and on the roles of other residues in the active site, will be forthcoming from future research. Information on enolase should also be useful in understanding catalysis by related enzymes that also promote enolate formation in carboxylate substrates [24].

Acknowledgement

We are grateful to the National Institutes of Health for support of work on enolase through Grants GM35752 (GHR) and AR35186 (IR).

References and recommended reading

Papers of particular interest, published within the annual period of review, have been highlighted as:

- • of special interest
- •• of outstanding interest

1. Dinovo EC, Boyer PD: **Isotopic probes of the enolase reaction mechanism.** *J Biol Chem* 1971, **246**:4586–4593.

2. Anderson SR, Anderson VE, Knowles JR: **Primary and secondary kinetic isotope effects as probes of the mechanism of yeast enolase.** *Biochemistry* 1994, **33**:10545–10555.

3. Anderson VE, Weiss PM, Cleland WW: **Reaction intermediate analogues for enolase.** *Biochemistry* 1984, **23**:2779–2786.

4. Stubbe J, Abeles RH: **Mechanism of action of enolase: effect of the β-hydroxy group on the rate of dissociation of the α-carbon-hydrogen bond.** *Biochemistry* 1980, **19**:5505–5512.

5. Shen TYS, Westhead EW: **Divalent cation and pH-dependent primary isotope effects in the enolase reaction.** *Biochemistry* 1973, **12**:3333–3337.

6. Anderson VE: **The mechanism of yeast enolase. [PhD Thesis].** Wisconsin: University of Wisconsin–Madison; 1981.

7. Burbaum JJ, Knowles JR: **Internal thermodynamics of enzymes determined by equilibrium quench: values of K_{int} for enolase and creatine kinase.** *Biochemistry* 1989, **28**:9306–9317.

8. Cohn M, Pearson JE, O'Connell EL, Rose IA: **Nuclear magnetic resonance assignment of the vinyl hydrogens of phosphoenolpyruvate. Stereochemistry of the enolase reaction.** *J Am Chem Soc* 1970, **92**:4095–4098.

9. Faller LD, Baroudy BM, Johnson AM, Ewall RX: **Magnesium ion requirements for yeast enolase activity.** *Biochemistry* 1977, **16**:3864–3869.

10. Chien JCW, Westhead EW: **Electron paramagnetic resonance study of the interaction of yeast enolase with activating metal ions.** *Biochemistry* 1971, **10**:3198–3203.

11. Poyner RR, Reed GH: **Structure of the *bis* divalent cation complex with phosphonoacetohydroxamate at the active site of enolase.** *Biochemistry* 1992, **31**:7166–7173.

12. Wedekind JE, Poyner RR, Reed GH, Rayment I: **Chelation of serine 39 to Mg^{2+} latches a gate at the active site of enolase: structure of the bis (Mg^{2+}) complex of yeast enolase and the intermediate analog phosphonoacetohydroxamate at 2.1 Å resolution.** *Biochemistry* 1994, **33**:9333–9342.

13. Lebioda L, Stec B, Brewer JM: **The structure of yeast enolase at 2.25 Å resolution.** *J Biol Chem* 1989, **264**:3685–3693.

14. •• Larsen TM, Wedekind JE, Rayment I, Reed GH: **A carboxylate oxygen of the substrate bridges the magnesium ions at the active site of enolase: structure of the yeast enzyme complexed with the equilibrium mixture of 2-phosphoglycerate and phosphoenolpyruvate at 1.8 Å resolution.** *Biochemistry* 1996, **35**:4349–4358.
The structure at 1.8 Å resolution of the cocrystallized complex of an equilibrium mixture of enolase with Mg^{2+} is presented. Data for this structure were collected from a crystal which was flash frozen at 160°C. Crystals were obtained from solutions at pH 8.0 from PEG. Difference electron density (F_o–F_c) shows the positions of the phosphate and carboxylate groups of the substrate/product, and strong density is present for the hydroxymethyl group of 2-PGA. This structure establishes the stereochemistry of substrate binding and coordination of both magnesium ions.

15. Wedekind JE, Reed GH, Rayment I: **Octahedral coordination at the high affinity metal site in enolase: crystallographic analysis of the Mg^{II}-enzyme complex from yeast at 1.9 Å resolution.** *Biochemistry* 1995, **34**:4325–4330.

16. Lebioda L, Stec B: **Mechanism of enolase: the crystal structure of enolase-Mg^{2+}-2-phosphoglycerate/phosphoenolpyruvate complex at 2.2 Å resolution.** *Biochemistry* 1991, **30**:2817–2822.

17. Duquerroy S, Camus C, Janin J: **X-ray structure and catalytic mechanism of lobster enolase.** *Biochemistry* 1995, **34**:12513–12523.

18. Brewer JM, Robson RL, Glover CV, Holland MJ, Lebioda L: **Preparation and characterization of the E168Q site-directed mutant of yeast enolase 1.** *Proteins* 1993, **17**:426–434.

19. • Sangadala VS, Glover GVC, Robson RL, Holland MJ, Lebioda L, Brewer JM: **Preparation by site-directed mutagenesis and characterization of the E211Q mutant of yeast enolase 1.** *Biochem Biophys Acta* 1995, **1251**:23–31.
The is the first report on the properties of Glu211Gln enolase. The mutant enzyme was purified from a yeast expression system. The data show a strong UV difference spectrum characteristic of the ionized form of TSP. A smaller change in the UV spectrum which developed after a significant time delay was interpreted as the ionization step. Experimental results in the TSP assay are in agreement with those reported for Glu211Gln enolase purified from the *E. coli* expression system [20••].

20. •• Poyner RR, Laughlin LT, Sowa GA, Reed GH: **Toward identification of acid/base catalysts in the active site of enolase: comparison of the properties of K345A, E168Q, and E211Q variants.** *Biochemistry* 1996, **35**:1692–1699.
This paper reports on the properties of Glu168Gln, Glu211Gln, and Lys345Ala enolases in the overall reaction, the H/D exchange in 2-PGA, the ionization of TSP and the hydrolysis of (Z)-3-Cl-phosphoenolpyruvate. The data show that Glu211Gln enolase is highly effective in the H/D exchange reaction, but much slower than wild type or the other variants in the hydrolysis of (Z)-3-Cl-phosphoenolpyruvate. This was the first evidence for the involvement of Glu211 in general-acid catalysis of the second step of enolase catalysis. The facile catalysis of the exchange reaction by Glu211Gln enolase provides additional support for the stepwise mechanism of enolase. The failure of Lys345Ala enolase to catalyze the H/D exchange reaction provided strong evidence for the action of Lys345 in general-base catalysis.

21. Stubbe J, Kenyon GL: **Analogs of phosphoenolpyruvate. Substrate specificities of enolase and pyruvate kinase from rabbit muscle.** *Biochemistry* 1972, **11**:338–345.

22. Terrill JB, Reilley CN: **Base-catalyzed hydrogen-deuterium exchange in bivalent metal-EDTA chelates.** *Anal Chem* 1966, **38**:1876–1881.

23. Hilal SH, Brewer JM, Lebioda L, Carreira LA: **Calculated effects of the chemical environment of 2-phospho-D-glycerate on the pK_a of its carbon-2 and correlations with the proposed mechanism of action of enolase.** *Biochem Biophys Res Commun* 1995, **211**:607–613.

24. Babbitt PC, Mrachko GT, Hasson MS, Huisman GW, Kolter R, Ringe D, Petsko GA, Kenyon GL, Gerlt JA: **A functionally diverse enzyme superfamily that abstracts the alpha protons of carboxylic acids.** *Science* 1995, **267**:1159–1161.

25. Kraulis PJ: **MOLSCRIPT: a program to produce both detailed and schematic plots of protein structures.** *J Appl Crystallogr* 1991, **24**:946–950.

26. Bacon DJ, Anderson WF: **A fast algorithm for rendering space-filling molecule pictures.** *J Mol Graphics* 1988, **6**:219–220.

27. Merritt EA, Murphy MEP: **Raster3D Version 2.0: a program for photorealistic molecular graphics.** *Acta Crystallogr D* 1994, **50**:869–873.